CHEMICAL PHYSICS

Unprecedented accuracy in molecular line-intensity ratios from frequency-based measurements

Jin-Ke Li[1,2]†, Jin Wang[1]†, Rui-Heng Yin[3], Qi Huang[3], Yan Tan[1,3]*, Chang-Le Hu[1,3], Yu R. Sun[4], Oleg L. Polyansky[5], Nikolai F. Zobov[5], Evgenii I. Lebedev[3], Rainer Stosch[6], Jonathan Tennyson[5]*, Gang Li[6], Shui-Ming Hu[1,2,3]*

Accurate determination of molecular transition intensities is vital to quantum chemistry and metrology, yet even simple diatomic molecules have historically been limited to 0.1% accuracy. Here, we show that frequency-domain measurements of relative intensity ratios outperform absolute methods, achieving 0.003% accuracy using dual-wavelength cavity mode dispersion spectroscopy. Enabled by high-precision frequency metrology, this approach reveals systematic discrepancies with state-of-the-art ab initio calculations, exposing subtle electron correlation effects in the dipole moment curve. Applied to line-intensity ratio thermometry (LRT), our technique determines gas temperatures with 0.5 millikelvin statistical uncertainty, exceeding previous LRT precision by two orders of magnitude. These results redefine the limits of optical gas metrology and enable International System of Units–traceable measurements for applications from combustion diagnostics to isotopic analysis. Discrepancies of up to 0.02% in transition probability ratios challenge theorists to refine models, establishing intensity ratios as a paradigm in precision molecular physics.

INTRODUCTION

Accurate knowledge of molecular transition intensities is essential for a wide range of applications, from remote sensing of planetary atmospheres (*1*–*3*) to precision tests of quantum chemistry calculations (*4*). However, as an intensity-dependent quantity, the precise determination of transition strengths—both experimentally and theoretically—remains a formidable challenge. Experimentally, high-precision measurements require rigorous control over thermodynamic conditions (temperature and pressure) and various instrumental factors, such as path length, pressure, and detector response (*5*). The line profile model that interprets the complicated collision-induced effect also presents a major difficulty (*6*) in retrieving line-intensity values from the observed spectra. Theoretically, the challenge lies in achieving sufficient accuracy in both the molecular wave functions and the dipole moment surfaces governing the transitions. Ab initio theory has proved to be highly accurate in predicting vibration-rotation transition intensities for simple diatomic molecules such as carbon monoxide (*7*–*9*) and molecular hydrogen (*10*, *11*). The unprecedented accuracy of these calculations has recently been demonstrated by comparing the predicted theoretical absolute intensities to measurements made in different laboratories (*12*–*15*), showing discrepancies below 0.1%.

However, the relative intensities of transitions, rather than their absolute values, are of greater importance in many applications. Examples include isotope ratio measurements in geochemistry (*16*), temperature diagnostics in combustion physics (*17*), and fundamental symmetries tests in molecular spectra (*18*). Relative intensity ratios benefit from the cancellation of common-mode systematic drifts, offering a pathway toward higher experimental precision. Theoretically, semi-empirical models can also exploit this cancellation to reduce uncertainties. Yet, despite these advantages, neither experiments nor theory have achieved relative intensity accuracies below the 0.01% threshold—a limitation that currently hinders key applications in precision spectroscopy and metrology.

Line-intensity ratio thermometry (LRT) (*19*–*22*) is an important application of relative intensity measurements by determining the gas temperature from the spectra of two optical transitions of the same molecule. Among the various techniques for thermodynamic temperature measurement (*23*), LRT provides direct traceability to the Boltzmann constant k_B, linking it to the definition of kelvin under the International System of Units (SI) (*24*). LRT inherently mitigates many systematic errors by measuring the ratio of two transitions, offering a substantial advantage over Doppler broadening thermometry (DBT) (*25*, *26*) in terms of accuracy and reproducibility. Despite its advantages, LRT has two key limitations as a primary thermometry method: High-precision [parts per million (ppm)–level] experimental measurements remain challenging, and its accuracy heavily relies on theoretical models of transition intensity ratios, where deviations can introduce systematic biases (*22*).

This work addresses both experimental and theoretical challenges by demonstrating LRT at the ppm level. Through frequency-based spectroscopy and refined semi-empirical modeling, we identify systematic deviations from prior state-of-the-art ab initio calculations (*7*). We demonstrate convergence between theory and experiment at the 3×10^{-5} level for vibration-rotation line-strength ratios—a 30-fold improvement over existing 0.1% absolute intensity benchmarks (*7*, *12*, *13*, *27*, *28*). This unprecedented agreement highlights the synergistic progress in both theoretical and experimental approaches. These advances not only enhance SI-traceable gas metrology (*29*, *30*) but also pinpoint specific areas for refinement in ab initio calculations, paving the way for next-generation primary thermometry standards.

[1]Hefei National Laboratory, University of Science and Technology of China, Hefei 230088, China. [2]State Key Laboratory of Chemical Reaction Dynamics, Department of Chemical Physics, University of Science and Technology of China, Hefei 230026, China. [3]Hefei National Research Center for Physical Sciences at the Microscale, University of Science and Technology of China, Hefei 230026, China. [4]Institute of Advanced Light Source Facilities, Shenzhen, 518107, China. [5]Department of Physics and Astronomy, University College London, Gower St, London WC1E 6BT, UK. [6]Physikalisch-Technische Bundesanstalt (PTB), Bundesallee 100, Braunschweig 38116, Germany.
*Corresponding author. Email: tanyan@ustc.edu.cn (Y.T.); j.tennyson@ucl.ac.uk (J.T.); smhu@ustc.edu.cn (S.-M.H.)
†These authors contributed equally to this work.

RESULTS

Dual-wavelength cavity mode dispersion spectroscopy (DW-CMDS) was used to determine the intensity ratio of two individual $^{12}C^{16}O$ lines. The CMDS method exploits the dispersion profile of a high-finesse optical cavity by measuring the frequency shifts in the cavity modes induced by molecular absorption, where both spectral axes correspond to precisely measurable frequencies, significantly reducing systematic errors such as detector nonlinearities (*31*, *32*). The setup, an upgrade from our previous implementations (*13*, *15*, *33*), used two lasers simultaneously locked to the cavity. The principle of the method and the experimental configuration are shown in Fig. 1, and additional experimental details are provided in the Supplementary Materials.

Figure 2A shows CMDS spectra of the R(5) and P(5) lines recorded with a sample pressure of 3.29 Pa. The spectra were fitted with the speed-dependent Voigt profile, and the center frequencies and integrated areas of both lines were derived from the fitting. More details of the fitting procedure are presented in the Supplementary Materials. The line-intensity ratio S_1 / S_2 at the experimental temperature was obtained from the observed spectra. Figure 2B shows the areas of R(5) and P(5) lines obtained from the spectra recorded in 7 hours. We can see drifts of the areas of both lines, but the drift disappears in the line-intensity ratios, as illustrated by the Allan deviation plot given in Fig. 2C. Figure 2D presents the intensity ratios of the R(5) and P(5) lines measured at different sample pressures and temperatures. At each pressure, the results were averaged over 600 scans recorded within 2 hours. As shown in Fig. 2, no difference could be evidenced in the results, indicating excellent consistency across the experimental conditions.

In total, we measured 24 pairs of CO transitions using the DW-CMDS method under pressures in the range of 3 to 648 Pa. The typical fractional uncertainty of the experimental ratios is 3×10^{-5}, primarily attributed to statistical uncertainty. A list of the results is given in the Supplementary Materials. We verified the consistency and reproducibility of our measurements using a "circulating ratios" test. We measured the following line-intensity ratios in separated measurements: R(1)/R(3), R(3)/R(5), R(5)/R(10), and R(1)/R(10). The first three are 0.535362(15), 0.769045(18), and 1.080442(17), which can be used to derive the line-intensity ratio of R(1)/R(10) as: $\frac{S_{R(1)}}{S_{R(10)}} = \frac{S_{R(1)}}{S_{R(3)}} \times \frac{S_{R(3)}}{S_{R(5)}} \times \frac{S_{R(5)}}{S_{R(10)}} = 0.444837(18)$, which agrees excellently with the directly measured experimental value of 0.444846(10).

DISCUSSION

Comparison with calculations

The intensity of a rovibrational transition at temperature T, which can be experimentally determined as the integrated absorbance divided by the molecular number density, is given by (*34*, *35*)

$$S = \frac{n_a g' A}{8\pi c \tilde{\nu}^2 Q(T)} \exp\left(-\frac{E}{k_B T}\right)\left[1 - \exp\left(-\frac{hc\tilde{\nu}}{k_B T}\right)\right] \quad (1)$$

where h is the Planck constant, c is the speed of light, k_B is the Boltzmann constant, n_a is the isotopolog abundance, g' is the statistical weight of the upper state, A is the Einstein-A coefficient, $Q(T)$ is the partition function (*36*), $\tilde{\nu}$ is the transition frequency in wave number, and E is the lower-state energy. For vibration-rotation transitions of the $^{12}C^{16}O$ molecule, we have $g' = 2J' + 1$, where J' is the rotational quantum number of the upper state.

Therefore, the experimentally measured line-intensity ratio of two lines relates to the ratio of their Einstein-A coefficients. For two near-infrared transitions ($hc\tilde{\nu} \gg k_B T$) of a molecule, the line-intensity ratio can be further simplified as (see the Supplementary Materials)

$$\frac{I_1}{I_2} = \frac{\tilde{\nu}_2^2 g_{1'} A_1}{\tilde{\nu}_1^2 g_{2'} A_2} \exp\left(\frac{E_2 - E_1}{k_B T}\right) \quad (2)$$

For the CO molecule, the lower-state energies and transition frequencies have been determined with very high accuracy (*37*). If the temperature is known, the experimentally measured line-intensity

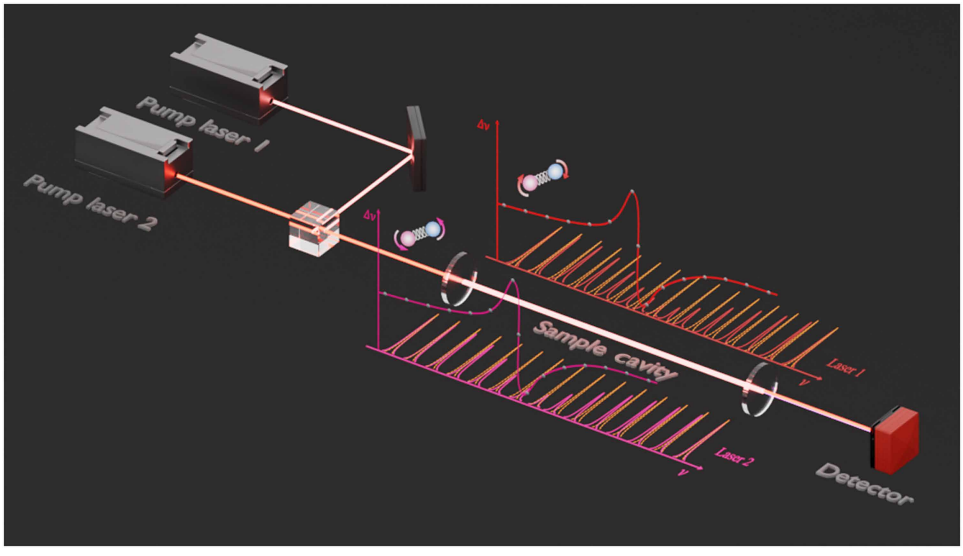

Fig. 1. Schematic diagram of DW-CMDS. Two rotation-vibration transitions measured simultaneously by dual-wavelength cavity-enhanced dispersion spectroscopy. Two lasers were coupled into a high-finesse cavity, scanning around two different molecular transitions. Cavity modes around each molecular transition are shifted from their original equally spaced positions (dark yellow curves). Dispersion spectra of both transitions were obtained by measuring the frequency shift ($\Delta\nu$) of each mode.

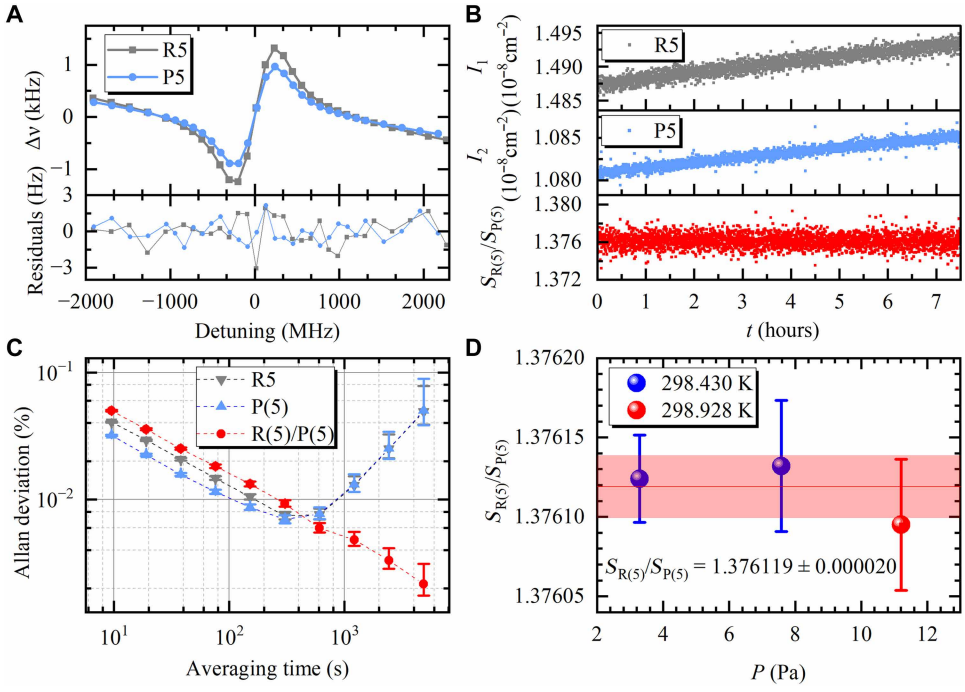

Fig. 2. Line-intensity ratio of two CO transitions measured by DW-CMDS. (**A**) Dispersion spectrum of the R(5) (gray) and P(5) (blue) lines and the fitting residuals. A single scan measured under 3.29 Pa. Speed-dependent Voigt (SDV) profile was used in fitting. (**B**) Integrated absorption areas of R(5) (black dots) and P(5) (blue dots) derived from the fitting. Their ratios are shown in red dots. (**C**) Allan deviations of $I_{R(5)}$, $I_{P(5)}$, and $I_{R(5)}$ / $I_{P(5)}$, normalized to the mean values and shown in %. (**D**) Line-intensity ratios of R(5)/P(5) obtained at different gas pressures and temperatures.

ratio can be used to derive the ratio of the Einstein-*A* coefficients, or conversely, to determine the temperature if the Einstein-*A* ratios have been well characterized for two transitions originating from different lower states. Note that the ratio of R(*J*)/P(*J*) from the same rotation state should be independent on temperature according to Eq. 2.

Using the experimental line-intensity ratios obtained in this work, we derived an empirical model of the Einstein-*A* ratios of transitions through a fitting (see the Supplementary Materials)

$$A = C_0 \frac{\tilde{\nu}^3 |m|}{2J'+1}\left(1+\frac{m}{C_1}+\frac{m^2}{C_2}+\frac{m^3}{C_3}\right)^2 \quad (3)$$

where the quantum number m is characterized as $J+1$ for an R(*J*) transition and $-J$ for a P(*J*) transition, with J' representing the rotational quantum number in the upper state. The coefficients $C_1 = 169.0628$, $C_2 = 30,966$, and $C_3 = 16,883,000$ were obtained through fitting, and C_0 is a fixed constant unaffected by m. This empirical formulation accurately predicts ratios of the Einstein-*A* coefficients, achieving a fractional deviation of 2.6×10^{-5}, which aligns with the experimental uncertainties. Figure 3 illustrates the deviations of the experimental results from the empirical model, with detailed numerical data available in the Supplementary Materials.

As part of this work, the University College London team performed revised ab initio calculations (hereafter UCL2025), showing notable improvements over their previous work (UCL2022) (*7*). While UCL2022 agreed with absolute line intensities at the 0.1% level (*7*, *12*), UCL2025 shows better agreement with line-intensity ratios observed in this work. Figure 3B reveals systematic discrepancies of approximately 0.2% between UCL2022 (pink line) and our empirical model (dashed line), particularly for P-branch lines. UCL2025 (cyan line) reduces these deviations to <0.02%, representing a more than 10-fold improvement. The temperature-independent R(*J*)/P(*J*) pairs (Fig. 3C) provide stringent tests of the calculations. UCL2025 agrees with the empirical model within the experimental uncertainty, while UCL2022 shows larger discrepancies (displayed at 1/10 scale in Fig. 3C for clarity). Similarly, R(*J*)/R($J+N$) ratios ($N = 1, 2$, Fig. 3D) demonstrate UCL2025's better consistency with empirical and experimental results across all rotational lines. Details of the calculations are provided in the Supplementary Materials.

The CCQM-P229 models (*12*) (represented by green and orange curves in Fig. 3B) exhibit systematic deviations of approximately 0.1% from our experimental results, regardless of the "dip correction" implementation. Notably, these deviation patterns display different characteristics compared to the UCL2022 predictions. Our comprehensive comparison with the previous state-of-the-art ab initio approach (*7*) and experimental benchmarks (*12*) on absolute line intensities reveals consistent discrepancies surpassing the 0.2% significance level.

This study represents, to our knowledge, the most precise experimental determination of molecular line-intensity ratios achieved to date, reaching an unprecedented accuracy at the 10^{-5} level. The persistent deviations observed among various theoretical approaches—including both ab initio calculations and empirical models—underscore critical challenges in current computational methodologies. These findings provide valuable benchmarks for improving first-principles calculations, particularly in treating the dipole moment curve (DMC) and quantum effects usually neglected in standard ab initio procedures.

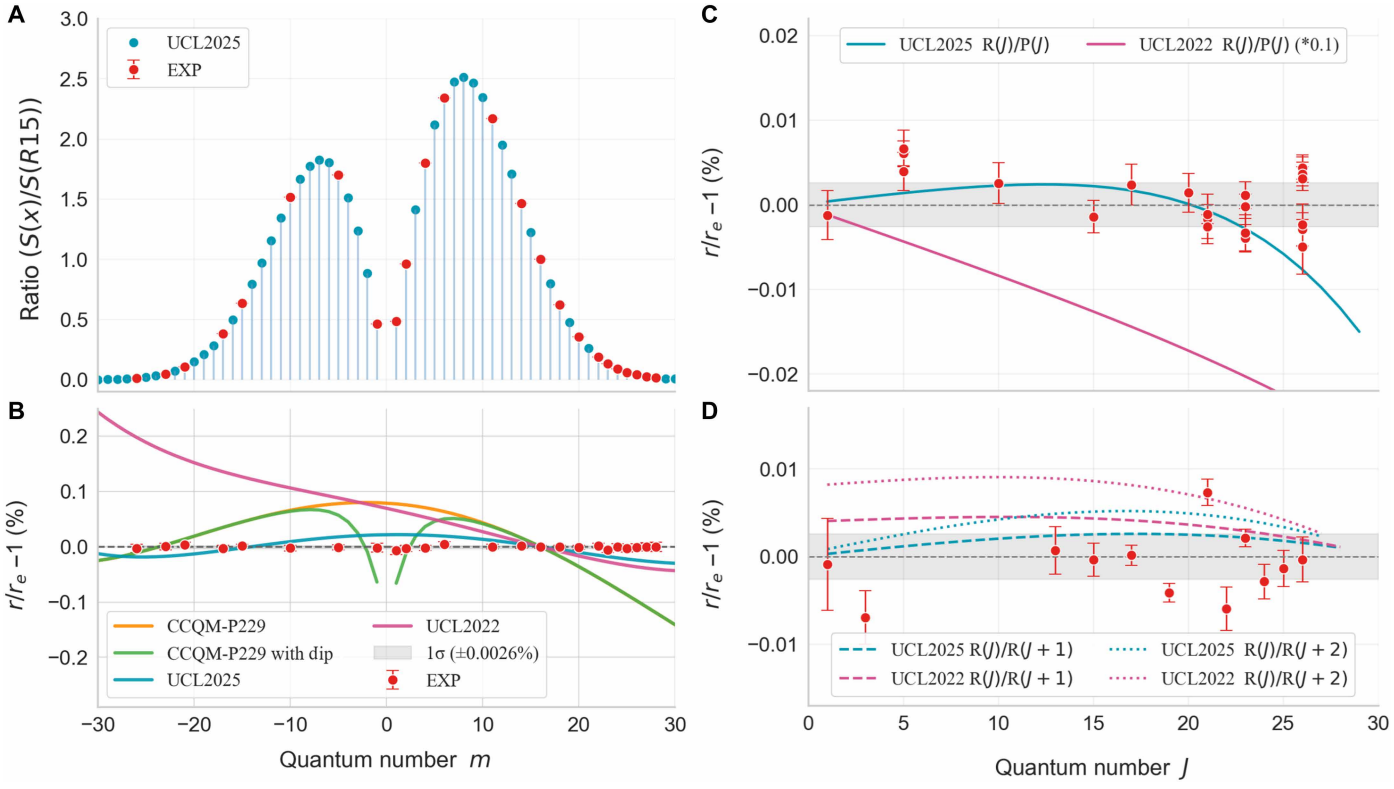

Fig. 3. Line intensities in the (3-0) vibrational band of $^{12}C^{16}O$ at 296 K. Red dots with error bars represent experimental results from this work. (**A**) and (**B**) show intensity ratios against the R(15) line. The quantum number *m* is defined as *–J* for P branch lines and *J* + 1 for R branch lines, where *J* is the rotational quantum number. (B) shows the deviations against the empirical model (Eq. 3) values (r_e). The cyan and pink curves represent the UCL2025 and UCL2022 ab initio calculated results, respectively. Orange and green lines represent the uncorrected CCQM-P229 reference values and those with dip correction, respectively (*12*). (**C**) Intensity ratios of the R(*J*)/P(*J*) line pairs, compared to the empirical model ratios (r_e). Cyan and pink lines represent the UCL2025 and UCL2022 results, respectively. The UCL2022 deviations are displayed at 1/10 scale, exceeding 0.2% for *J* > 20. (**D**) Intensity ratios of R(*J*)/R(*J* + 1) (dashed lines) and R(*J*)/R(*J* + 2) (dotted lines), compared to the empirical model ratios (r_e). Cyan and pink colors represent UCL2025 and UCL2022. Gray belts indicate the 1σ uncertainty of the empirical ratios.

A particular challenge on the theory side is to determine why the UCL2022 model works better than the UCL2025 model presented here for absolute intensities, while the UCL2025 model is superior for the intensity ratios. Undoubtedly, these differences are caused by the cancellation of errors. The two models use the same nuclear motion wave functions, usually thought of as accounting for small changes due to rotational state, but differ in the level of theory used to compute the ab initio DMC. It is necessary to explore further both the level of theory [complete active space (CAS), basis set convergence, and relativistic and quantum electrodynamic corrections] and possible corrections to the Born-Oppenheimer approximation. The unprecedented accuracy of the current experiments is posing questions for theory, which requires further investigation.

Line-intensity ratio thermometry

As a demonstration, we conducted LRT measurements at two distinct temperatures using two different line pairs. According to Eq. 2, the temperature sensitivity in LRT measurements relies on the difference between the lower-level energies of the transition pair

$$\frac{d(I_1/I_2)}{I_1/I_2} = -\frac{E_2 - E_1}{k_B T} \cdot \frac{dT}{T} = -\eta \frac{dT}{T} \quad (4)$$

where η is the coefficient factor. The LRT sensitivity can be considerably improved by selecting transitions with a larger η. For the R(1)/R(17) line pair, the lower-state energies are 3.8450 cm^{-1} and 587.7209 cm^{-1}, yielding $\eta_{R(1),R(17)} \simeq 2.8$. For the R(0)/R(20) pair, the lower-state energies are 0 and 806.3828 cm^{-1}, resulting in a higher enhancement factor of $\eta_{R(0),R(20)} \simeq 3.9$. An additional consideration in selecting transitions for LRT is that the intensities of the two lines should be comparable. This ensures that a reasonable gas pressure can be used to achieve a good signal-to-noise ratio for both transitions. For the R(1)/R(17) pair, the line-intensity ratio is approximately 1.55 around 298 K, while for the R(0)/R(20) pair, the ratio is 1.86.

Using Eq. 2 and empirical Einstein-*A* ratios (see Eq. 3 and the Supplementary Materials), we converted the measured line-intensity ratios into temperature values. For the R(1)/R(17) pair measured at 298.43 K and 16.2 Pa (Fig. 4A), the 5-hour averaged LRT result was 298.4315(11) K, deviating by 1.3 mK from the temperature of the sensor reading [298.4328(10) K]. An Allan deviation analysis (Fig. 4C) shows a relative uncertainty of 4×10^{-4} $Hz^{-1/2}$, improving to 6×10^{-6} (6 ppm) after 1 hour of averaging. The R(0)/R(20) pair measured at 298.93 K and 33.3 Pa (Fig. 4B) exhibited a slightly better performance, with an Allan deviation of 3×10^{-4} $Hz^{-1/2}$, attributed to its higher

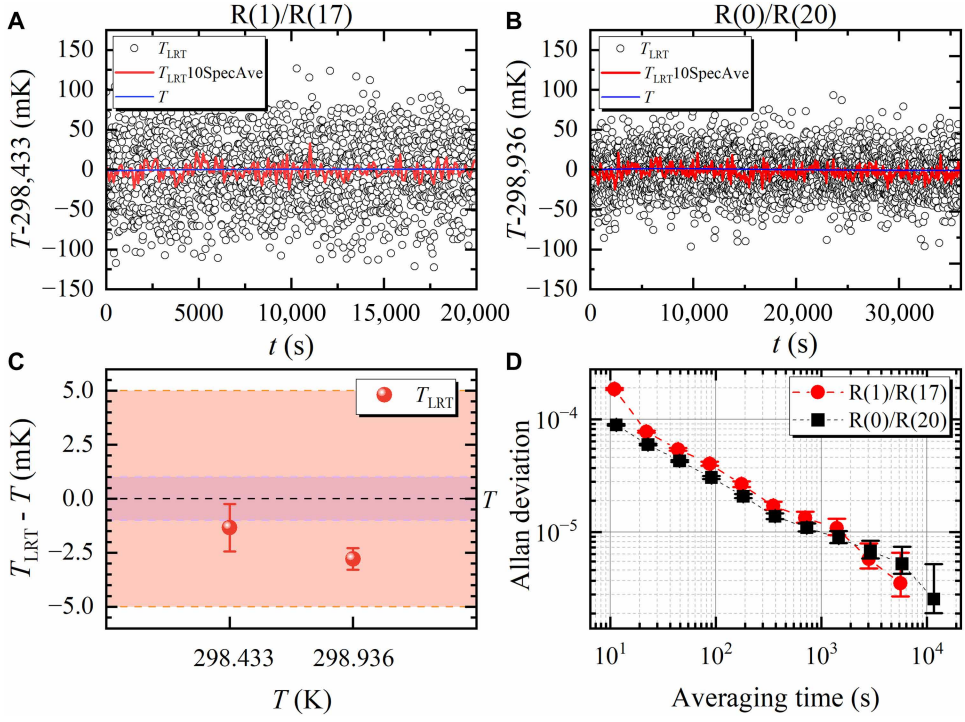

Fig. 4. Line-intensity ratio thermometry (LRT) demonstrated with line pairs of CO at different temperatures. (**A**) LRT temperature (T_{LRT}) using the R(1)/R(17) line pair. Black circles indicate results with a temporal resolution of 10 s per scan, and the red line shows the 10-scan averaged results. The blue line indicates the temperature (T) calibrated from the readings of platinum sensors. (**B**) LRT temperature using the R(0)/R(20) line pair. (**C**) Deviation between the temperatures obtained by LRT (T_{LRT}) and temperature of sensors (T). Pink and orange belts represent the drift and calibration errors of the platinum thermal sensors, respectively. (**D**) Allan deviation of $T_{LRT} / T - 1$.

enhancement factor η. The empirical Einstein-*A* coefficient ratio introduces a systematic uncertainty of 26 ppm, contributing 6.7 ppm to the LRT temperature uncertainty. In the 10-hour measurement with the R(0)/R(20) pair, the LRT-derived temperature was 298.9330 K with a statistical (type A) uncertainty of 0.5 mK and a systematic (type B) uncertainty of 2.0 mK. This agrees well with the temperature of the sensor reading of 298.9358(10) K, which has an additional 5 mK calibration uncertainty.

Figure 5 summarizes molecular spectroscopy–based thermometry results to date, alongside Boltzmann constant (k_B) determinations (uncertainty: 0.6 to 7 ppm) (*23*, *38*–*45*). The DBT method was pioneered by Daussy *et al.* (*25*) from Université Paris 13, followed by the Caserta group (*26*, *46*, *47*). Various transitions were used, including NH_3 in the mid-infrared (*25*, *48*), CO_2 (*26*), H_2O (*49*), and C_2H_2 (*29*, *47*, *50*, *51*) lines in the near-infrared, and also atomic Rb transitions (*52*, *53*). The best DBT result (14 ppm uncertainty, 33 ppm deviation) was achieved with CO_2 at 1578 nm (*54*). For LRT, key contributions include Shimizu *et al.* (Tsukuba) (*19*), Gotti *et al.* (Caserta) (*20*), and Lisak *et al.* (Toruń) (*55*). This work sets a benchmark: 1.7-ppm statistical uncertainty and 6.7-ppm systematic uncertainty, with <10-ppm deviation from platinum thermometer references. This represents the highest accuracy in optical thermometry to date.

Perspectives

DW-CMDS is a versatile methodology applicable to a broad spectrum of molecular species. By integrating phase-stabilized laser technology, all frequency-based measurements, and multiline fitting

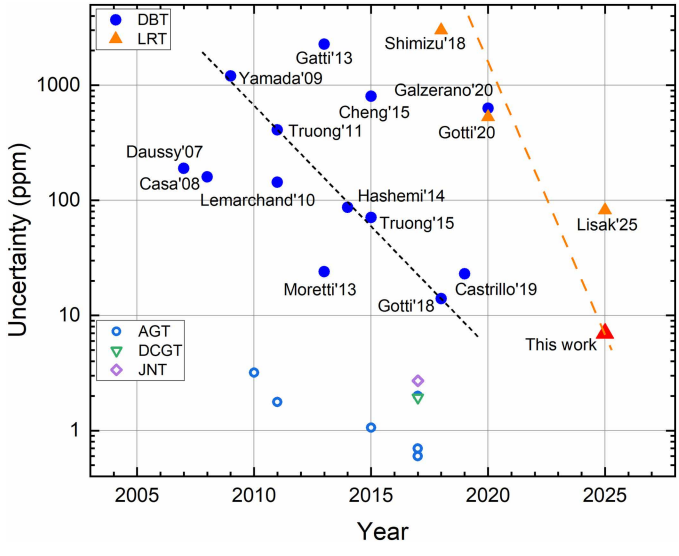

Fig. 5. Thermometry based on optical spectroscopy. Doppler-broadening thermometry (DBT): Daussy'07 (*25*), Casa'08 (*26*), Yamada'09 (*50*), Lemarchand'10 (*48*), Truong'11 (*52*), Moretti'13 (*49*), Hashemi'14 (*51*), Cheng'15 (*29*), Truong'15 (*53*), Gotti'18 (*54*), Castrillo'19 (*47*), and Galzerano'20 (*56*). Line-intensity ratio thermometry (LRT): Shimizu'18 (*19*), Gotti'20 (*20*), Lisak'25 (*55*), and this work. For comparison, the results included in the determination of the Boltzmann constant (*23*) are also shown here, including three methods: acoustic gas thermometry (AGT) (*38*–*43*), dielectric-constant gas thermometry (DCGT) (*44*), and Johnson noise thermometry (JNT) (*45*).

algorithms, this approach achieves metrological traceability in relative line-intensity ratio determinations with unprecedented sub-0.01% uncertainty—surpassing the precision limits of conventional optical methods. The exceptional accuracy of these measurements uncovers systematic inconsistencies with current ab initio predictions, exposing previously unrecognized limitations in our understanding of dipole moment surfaces and electron correlation effects—findings that will likely catalyze theoretical developments in quantum chemistry and molecular physics.

From a metrological perspective, the methodology's unique ability to analyze gas mixtures under extreme conditions overcomes persistent challenges in high-temperature metrology, where traditional methods suffer from thermal interference effects and impractical purity requirements. DW-CMDS introduces a transformative capability for direct, calibration-free determination of isotopolog abundance ratios with inherent SI traceability. This breakthrough has immediate implications for critical applications including atmospheric monitoring (particularly greenhouse gas quantification), nuclear safeguards, and next-generation reference material development. By providing a rigorous link between spectroscopic data and gravimetric standards, the technique offers National Metrology Institutes a pathway to establish more robust calibration and measurement capabilities while reducing dependence on physical reference materials susceptible to degradation.

The exceptional precision of DW-CMDS enables reliable in situ characterization of chemical composition and thermodynamic parameters in challenging environments such as combustion zones or plasma discharges. Moreover, its noninvasive nature and minimal sample preparation requirements align with current demands for high-throughput spectroscopic diagnostics in both fundamental research and industrial process monitoring.

MATERIALS AND METHODS

The experimental measurements were performed using DW-CMDS, a frequency-based technique that exploits the dispersion profile of a high-finesse optical cavity. Two external-cavity diode lasers were simultaneously locked to the cavity using the Pound-Drever-Hall technique, enabling precise measurement of frequency shifts induced by molecular absorption. The setup incorporated acousto-optic and electro-optic modulators to scan and resolve cavity modes, with frequencies referenced to a global positioning system (GPS)-calibrated rubidium clock. Spectra were recorded for 24 pairs of CO transitions at pressures ranging from 3 to 648 Pa and temperatures stabilized to ±1 mK. Line profiles were fitted with a speed-dependent Voigt model to extract integrated intensities, achieving a typical fractional uncertainty of 3×10^{-5} for intensity ratios. More experimental details are given in the Supplementary Materials.

To interpret the measurements, we developed an empirical model incorporating third-order Herman-Wallis factors, which reproduced experimental intensity ratios within 2.6×10^{-5} fractional deviation. Ab initio calculations were performed using the Duo program, solving the rovibrational Schrödinger equation with a refined DMC computed at the MRCI+Q/aug-cc-pCV6Z level. A 6220 CAS was selected, reducing discrepancies with experimental line-intensity ratios to the level of 0.02%. More details of the theoretical calculations are provided in the Supplementary Materials.

Supplementary Materials

This PDF file includes:

Experimental Line-Intensity Ratios
Empirical Model
AB Initio Calculations
Figs. S1 to S5
Tables S1 and S2
References

REFERENCES AND NOTES

1. D. J. Des Marais, M. O. Harwit, K. W. Jucks, J. F. Kasting, D. N. C. Lin, J. I. Lunine, J. Schneider, S. Seager, W. A. Traub, N. J. Woolf, Remote sensing of planetary properties and biosignatures on extrasolar terrestrial planets. *Astrobiology* **2**, 153–181 (2002).
2. O. L. Polyansky, K. Bielska, M. Ghysels, L. Lodi, N. F. Zobov, J. T. Hodges, J. Tennyson, High-accuracy CO_2 line intensities determined from theory and experiment. *Phys. Rev. Lett.* **114**, 243001 (2015).
3. E. Roueff, H. Abgrall, P. Czachorowski, K. Pachucki, M. Puchalski, J. Komasa, The full infrared spectrum of molecular hydrogen. *Astron. Astrophys.* **630**, A58 (2019).
4. C. W. Bauschlicher Jr., S. R. Langhoff, P. R. Taylor, in *Accurate Quantum Chemical Calculations* (John Wiley & Sons, Ltd., 1990), pp. 103–161.
5. A. J. Fleisher, E. M. Adkins, Z. D. Reed, H. Yi, D. A. Long, H. M. Fleurbaey, J. T. Hodges, Twenty-five-fold reduction in measurement uncertainty for a molecular line intensity. *Phys. Rev. Lett.* **123**, 043001 (2019).
6. H. Tran, C. Boulet, J. Hartmann, Line mixing and collision-induced absorption by oxygen in the A band: Laboratory measurements, model, and tools for atmospheric spectra computations. *J. Geophys. Res. Atmos.* **111**, D15210 (2006).
7. K. Bielska, A. A. Kyuberis, Z. D. Reed, G. Li, A. Cygan, R. Ciuryło, E. M. Adkins, L. Lodi, N. F. Zobov, V. Ebert, D. Lisak, J. T. Hodges, J. Tennyson, O. L. Polyansky, Subpromille measurements and calculations of CO (3-0) overtone line intensities. *Phys. Rev. Lett.* **129**, 043002 (2022).
8. A. A. Balashov, K. Bielska, G. Li, A. A. Kyuberis, S. Wójtewicz, J. Domysławska, R. Ciuryło, N. F. Zobov, D. Lisak, J. Tennyson, O. L. Polyansky, Measurement and calculation of CO (7–0) overtone line intensities. *J. Chem. Phys.* **158**, 234306 (2023).
9. N. F. Zobov, R. I. Ovsyannikov, M. A. Rogov, E. I. Lebedev, J. Tennyson, O. L. Polyansky, CO line intensities: Towards subpercent accuracy of intensities of all bands. *J. Quant. Spectrosc. Radiat. Transf.* **325**, 109510 (2025).
10. J. Komasa, M. Puchalski, P. Czachorowski, G. Lach, K. Pachucki, Rovibrational energy levels of the hydrogen molecule through nonadiabatic perturbation theory. *Phys. Rev. A* **100**, 032519 (2019).
11. M. Puchalski, J. Komasa, P. Czachorowski, K. Pachucki, Nonadiabatic QED correction to the dissociation energy of the hydrogen molecule. *Phys. Rev. Lett.* **122**, 103003 (2019).
12. J. T. Hodges, K. Bielska, M. Birk, R. Guo, G. Li, J. S. Lim, D. Lisak, Z. D. Reed, G. Wagner, International comparison CCQM-P229 pilot study to measure line intensities of selected $^{12}C^{16}O$ transitions. *Metrologia* **62**, 08006 (2025).
13. Q. Huang, Y. Tan, R. H. Yin, Z. L. Nie, J. Wang, S. M. Hu, Line intensities of CO near 1560 nm measured with absorption and dispersion spectroscopy. *Metrologia* **61**, 065003 (2024).
14. H. Fleurbaey, A. Koroleva, S. Kassi, A. Campargue, The high accuracy spectroscopy of H2 rovibrational transitions in the (2-0) band near 1.2 μm. *Phys. Chem. Chem. Phys.* **25**, 14749–14756 (2023).
15. H. Liang, Y. Tan, C. L. Hu, Z. L. Nie, A. W. Liu, Y. R. Sun, J. Wang, S. M. Hu, Cavity-enhanced absorption and dispersion spectroscopy of the 1238-nm line of H_2. *Phys. Rev. A* **110**, 042817 (2024).
16. A. J. Fleisher, H. Yi, A. Srivastava, O. L. Polyansky, N. F. Zobov, J. T. Hodges, Absolute $^{13}C/^{12}C$ isotope amount ratio for Vienna PeeDee Belemnite from infrared absorption spectroscopy. *Nat. Phys.* **17**, 889–893 (2021).
17. M. Aldén, Spatially and temporally resolved laser/optical diagnostics of combustion processes: From fundamentals to practical applications. *Proc. Combust. Inst.* **39**, 1185–1228 (2023).
18. M. Quack, F. Merkt, eds., in *Fundamental Symmetries and Symmetry Violations from High Resolution Spectroscopy* (Wiley, 2011), pp. 659–722.
19. Y. Shimizu, S. Okubo, A. Onae, K. M. T. Yamada, H. Inaba, Molecular gas thermometry on acetylene using dual-comb spectroscopy: Analysis of rotational energy distribution. *Appl. Phys. B* **124**, 71 (2018).
20. R. Gotti, M. Lamperti, D. Gatti, S. Wójtewicz, T. Puppe, Y. Mayzlin, B. Alsaif, J. Robinson-Tait, F. Rohde, R. Wilk, P. Leisching, W. G. Kaenders, P. Laporta, M. Marangoni, Multispectrum rotational states distribution thermometry: Application to the $3\nu_1 + \nu_3$ band of carbon dioxide. *New J. Phys.* **22**, 083071 (2020).
21. L. Santamaria, M. S. D. Cumis, D. Dequal, G. Bianco, C. P. Pablo, A new precision spectroscopy based method for Boltzmann constant determination and primary thermometry. *J. Phys. Chem. A* **122**, 6026–6030 (2018).

22. R. Gotti, M. Lamperti, D. Gatti, M. Marangoni, Laser-based primary thermometry: A review. *J. Phys. Chem. Ref. Data Monogr.* **50**, 031501 (2021).
23. J. Fischer, B. Fellmuth, C. Gaiser, T. Zandt, L. Pitre, F. Sparasci, M. D. Plimmer, M. de Podesta, R. Underwood, G. Sutton, G. Machin, R. M. Gavioso, D. Madonna Ripa, P. P. M. Steur, J. Qu, X. J. Feng, J. Zhang, M. R. Moldover, S. P. Benz, D. R. White, L. Gianfrani, A. Castrillo, L. Moretti, B. Darquié, E. Moufarej, C. Daussy, S. Briaudeau, O. Kozlova, L. Risegari, J. J. Segovia, M. C. Martín, D. del Campo, The Boltzmann project. *Metrologia* **55**, R1–R20 (2018).
24. M. Stock, R. Davis, E. de Mirandés, M. J. T. Milton, The revision of the SI—The result of three decades of progress in metrology. *Metrologia* **56**, 022001 (2019).
25. C. Daussy, M. Guinet, A. Amy-Klein, K. Djerroud, Y. Hermier, S. Briaudeau, C. J. Bordé, C. Chardonnet, Direct determination of the Boltzmann constant by an optical method. *Phys. Rev. Lett.* **98**, 250801 (2007).
26. G. Casa, A. Castrillo, G. Galzerano, R. Wehr, A. Merlone, D. di Serafino, P. Laporta, L. Gianfrani, Primary gas thermometry by means of laser-absorption spectroscopy: Determination of the Boltzmann constant. *Phys. Rev. Lett.* **100**, 200801 (2008).
27. V. V. Meshkov, A. Y. Ermilov, A. V. Stolyarov, E. S. Medvedev, V. G. Ushakov, I. E. Gordon, Semi-empirical dipole moment of carbon monoxide and line lists for all its isotopologues revisited. *J. Quant. Spectrosc. Radiat. Transf.* **280**, 108090 (2022).
28. A. Cygan, S. Wójtewicz, H. Jóźwiak, G. Kowzan, N. Stolarczyk, K. Bielska, P. Wcisło, R. Ciuryło, D. Lisak, Dispersive heterodyne cavity ring-down spectroscopy exploiting eigenmode frequencies for high-fidelity measurements. *Sci. Adv.* **11**, eadp8556 (2025).
29. C. F. Cheng, J. Wang, Y. R. Sun, Y. Tan, P. Kang, S. M. Hu, Doppler broadening thermometry based on cavity ring-down spectroscopy. *Metrologia* **52**, S385–S393 (2015).
30. G. Li, A. Röttger, M. Zboril, O. Werhahn, Metrology for climate action. *Meas. Sens.* **38**, 101850 (2025).
31. A. Cygan, P. Wcisło, S. Wójtewicz, P. Masłowski, J. T. Hodges, R. Ciuryło, D. Lisak, One-dimensional frequency-based spectroscopy. *Opt. Expr.* **23**, 14472 (2015).
32. A. Cygan, P. Wcisło, S. Wójtewicz, G. Kowzan, M. Zaborowski, D. Charczun, K. Bielska, R. S. Trawiński, R. Ciuryło, P. Masłowski, D. Lisak, High-accuracy and wide dynamic range frequency-based dispersion spectroscopy in an optical cavity. *Opt. Expr.* **27**, 21810–21821 (2019).
33. J. Wang, Y. R. Sun, L.-G. Tao, A.-W. Liu, S.-M. Hu, Communication: Molecular near-infrared transitions determined with sub-kHz accuracy. *J. Chem. Phys.* **147**, 091103 (2017).
34. M. Šimečková, D. Jacquemart, L. S. Rothman, R. Gamache, A. Goldman, Einstein A-coefficients and statistical weights for molecular absorption transitions in the HITRAN database. *J. Quant. Spectrosc. Radiat. Transf.* **98**, 130–155 (2006).
35. P. F. Bernath, *Spectra of Atoms and Molecules* (Oxford Univ. Press, 2016).
36. R. R. Gamache, B. Vispoel, M. Rey, A. Nikitin, V. Tyuterev, O. Egorov, I. E. Gordon, V. Boudon, Total internal partition sums for the HITRAN2020 database. *J. Quant. Spectrosc. Radiat. Transf.* **271**, 107713 (2021).
37. J. Wang, C. L. Hu, A. W. Liu, Y. R. Sun, Y. Tan, S. M. Hu, Saturated absorption spectroscopy near 1.57 μm and revised rotational line list of $^{12}C^{16}O$. *J. Quant. Spectrosc. Radiat. Transf.* **270**, 107717 (2021).
38. M. R. Moldover, J. P. M. Trusler, T. J. Edwards, J. B. Mehl, R. S. Davis, Measurement of the universal gas constant R using a spherical acoustic resonatore. *J. Res. Natl. Bur. Stand.* **93**, 85–144 (1988).
39. R. M. Gavioso, D. Madonna Ripa, P. P. M. Steur, C. Gaiser, D. Truong, C. Guianvarc'h, P. Tarizzo, F. M. Stuart, R. Dematteis, A determination of the molar gas constant R by acoustic thermometry in helium. *Metrologia* **52**, S274–S304 (2015).
40. L. Pitre, F. Sparasci, L. Risegari, C. Guianvarc'h, C. Martin, M. E. Himbert, M. D. Plimmer, A. Allard, B. Marty, P. A. Giuliano Albo, B. Gao, M. R. Moldover, J. B. Mehl, New measurement of the Boltzmann constant *k* by acoustic thermometry of helium-4 gas. *Metrologia* **54**, 856–873 (2017).
41. X. J. Feng, J. T. Zhang, H. Lin, K. A. Gillis, J. B. Mehl, M. R. Moldover, K. Zhang, Y. N. Duan, Determination of the Boltzmann constant with cylindrical acoustic gas thermometry: New and previous results combined. *Metrologia* **54**, 748–762 (2017).
42. J. J. Segovia, D. Lozano-Martín, M. C. Martín, C. R. Chamorro, M. A. Villamañán, E. Pérez, C. García Izquierdo, D. del Campo, Updated determination of the molar gas constant R by acoustic measurements in argon at UVa-CEM. *Metrologia* **54**, 663–673 (2017).
43. M. de Podesta, D. F. Mark, R. C. Dymock, R. Underwood, T. Bacquart, G. Sutton, S. Davidson, G. Machin, Re-estimation of argon isotope ratios leading to a revised estimate of the Boltzmann constant. *Metrologia* **54**, 683–692 (2017).
44. C. Gaiser, B. Fellmuth, N. Haft, A. Kuhn, B. Thiele-Krivoi, T. Zandt, J. Fischer, O. Jusko, W. Sabuga, Final determination of the Boltzmann constant by dielectric-constant gas thermometry. *Metrologia* **54**, 280–289 (2017).
45. J. Qu, S. P. Benz, K. Coakley, H. Rogalla, W. L. Tew, R. White, K. Zhou, Z. Zhou, An improved electronic determination of the Boltzmann constant by Johnson noise thermometry. *Metrologia* **54**, 549–558 (2017).
46. E. Fasci, M. Domenica de Vizia, A. Merlone, L. Moretti, A. Castrillo, L. Gianfrani, The Boltzmann constant from the H_2 ^{18}O vibration-rotation spectrum: Complementary tests and revised uncertainty budget. *Metrologia* **52**, S233–S241 (2015).
47. A. Castrillo, E. Fasci, H. Dinesan, S. Gravina, L. Moretti, L. Gianfrani, Optical determination of thermodynamic temperatures from a C_2H_2 line-doublet in the near infrared. *Phys. Rev. Appl.* **11**, 064060 (2019).
48. C. Lemarchand, K. Djerroud, B. Darquié, O. Lopez, A. Amy-Klein, C. Chardonnet, C. J. Bordé, S. Briaudeau, C. Daussy, Determination of the Boltzmann constant by laser spectroscopy as a basis for future measurements of the thermodynamic temperature. *Int. J. Thermophys.* **31**, 1347–1359 (2010).
49. L. Moretti, A. Castrillo, E. Fasci, M. D. de Vizia, G. Casa, G. Galzerano, A. Merlone, P. Laporta, L. Gianfrani, Determination of the Boltzmann constant by means of precision measurements of $H_2^{18}O$ line shapes at 1.39 μm. *Phys. Rev. Lett.* **111**, 060803 (2013).
50. K. M. T. Yamada, A. Onae, F.-L. Hong, H. Inaba, T. Shimizu, Precise determination of the Doppler width of a rovibrational absorption line using a comb-locked diode laser. *C. R. Phys.* **10**, 907–915 (2009).
51. R. Hashemi, C. Povey, M. Derksen, H. Naseri, J. Garber, A. Predoi-Cross, Doppler broadening thermometry of acetylene and accurate measurement of the Boltzmann constant. *J. Chem. Phys.* **141**, 214201 (2014).
52. G. W. Truong, E. F. May, T. M. Stace, A. N. Luiten, Quantitative atomic spectroscopy for primary thermometry. *Phys. Rev. A* **83**, 033805 (2011).
53. G. W. Truong, D. Stuart, J. D. Anstie, E. F. May, T. M. Stace, A. N. Luiten, Atomic spectroscopy for primary thermometry. *Metrologia* **52**, S324–S342 (2015).
54. R. Gotti, L. Moretti, D. Gatti, A. Castrillo, G. Galzerano, P. Laporta, L. Gianfrani, M. Marangoni, Cavity-ring-down Doppler-broadening primary thermometry. *Phys. Rev. A* **97**, 012512 (2018).
55. D. Lisak, V. D'Agostino, S. Wójtewicz, A. Cygan, M. Gibas, P. Wcisło, R. Ciuryło, K. Bielska, Leveraging resonant frequencies of an optical cavity for spectroscopic measurement of gas temperature and concentration. arXiv:2502.17660 [physics.optics] (2025).
56. G. Galzerano, Absolute temperature measurements by direct-frequency-comb spectroscopy. *Measurement* **164**, 107940 (2020).
57. R. Herman, R. F. Wallis, Influence of vibration-rotation interaction on line intensities in vibration-rotation bands of diatomic molecules. *J. Chem. Phys.* **23**, 637–646 (1955).
58. J. K. Watson, Quadratic Herman-Wallis factors in the fundamental bands of linear molecules. *J. Mol. Spectrosc.* **125**, 428–441 (1987).
59. S. N. Yurchenko, L. Lodi, J. Tennyson, A. V. Stolyarov, Duo: A general program for calculating spectra of diatomic molecules. *Comput. Phys. Commun.* **202**, 262–275 (2016).
60. I. I. Mizus, L. Lodi, J. Tennyson, N. F. Zobov, O. L. Polyansky, An analysis of the accuracy of line intensities calculations using DUO and LEVEL program package. *J. Mol. Spectrosc.* **368**, 111621 (2022).
61. H.-J. Werner, P. J. Knowles, G. Knizia, F. R. Manby, M. Schütz, Molpro: A general-purpose quantum chemistry program package. *WIREs Comput. Mol. Sci.* **2**, 242–253 (2012).
62. L. Lodi, J. Tennyson, Theoretical methods for small-molecule ro-vibrational spectroscopy. *J. Phys. B At. Mol. Opt. Phys.* **43**, 133001 (2010).
63. J. Koput, Toward accurate ab initio ground-state potential energy and 2 electric dipole moment functions of carbon monoxide. *J. Chem. Theo. Comput.* **20**, 9041–9047 (2024).
64. J. A. Coxon, P. G. Hajigeorgiou, Direct potential fit analysis of the $X^1\Sigma^+$ ground state of CO. *J. Chem. Phys.* **121**, 2992–3008 (2004).

Acknowledgments: O.L.P. acknowledges N. Ipfan for technical support. **Funding:** This work was jointly supported by the Independent Deployment Project of HFNL (grant no. ZB2025010500), the Innovation Program for Quantum Science and Technology (grant nos. 2021ZD0303102 and 2022YFF0606500), the National Natural Science Foundation of China (grant nos. 12393825 and 12393822), and the Chinese Academy of Sciences (XDB0970100). O.L.P., J.T., R.S., and G.L. acknowledge support from the project (22IEM03 PriSpecTemp), which has received funding from the European Partnership on Metrology, cofinanced by the European Union's Horizon Europe Research and Innovation Programme and by the participating states. J.T. and O.L.P. acknowledge support from ERC Advanced Investigator Project 883830 and the State Project IAP no. FFUF-2024-0016. **Author contributions:** J.-K.L. and J.W. contributed equally to this work and share first authorship, and S.-M.H. was the main project coordinator of the study. Conceptualization: Y.T., O.L.P., J.-K.L., J.W., C.-L.H., S.-M.H., and G.L. Investigation: Y.T., Y.R.S., J.-K.L., J.W., C.-L.H., S.-M.H., G.L., and J.T. Methodology: N.F.Z., Y.T., Y.R.S., O.L.P., J.-K.L., Q.H., S.-M.H., and J.T. Data curation: Y.T., J.-K.L., J.W., and J.T. Validation: N.F.Z., Y.T., O.L.P., J.W., E.I.L., and J.T. Formal analysis: R.S., Y.T., Y.R.S., O.L.P., J.-K.L., J.W., C.-L.H., S.-M.H., and E.I.L. Software: N.F.Z., Y.T., J.-K.L., J.W., R.-H.Y., and J.T. Visualization: N.F.Z., Y.T., J.-K.L., J.W., C.-L.H., and E.I.L. Writing—original draft: R.S., Y.T., O.L.P., J.-K.L., J.W., S.-M.H., and G.L. Writing—review and editing: R.S., Y.T., Y.R.S., J.-K.L., S.-M.H., G.L., and J.T. Supervision: Y.T., Y.R.S., J.W., S.-M.H., and J.T. Project administration: Y.T., J.W., S.-M.H., and G.L. Resources: Y.T., J.-K.L., S.-M.H., and J.T. Funding acquisition: Y.T., S.-M.H., G.L., and J.T. **Competing interests:** The authors declare that they have no competing interests. **Data and materials availability:** All data needed to evaluate the conclusions in the paper are present in the paper and/or the Supplementary Materials.

Submitted 9 June 2025
Accepted 19 August 2025
Published 17 September 2025
10.1126/sciadv.adz6560